Supporting Information

Morphology engineering of Atomic Layer Defect-Rich $CoSe_2$ Nanosheets for Highly Selective Electrosynthesis of Hydrogen Peroxide

Yuan Ji,[a] Yundan Liu,[a]* Bin-Wei Zhang,[b]* Zhongfei Xu,[c] Xiang Qi,[a] Xun Xu,[b] Long Ren,[e]* Yi Du,[b,d] Jianxin Zhong [a] and Shi Xue Dou[b,d]

[a] *Hunan Key Laboratory of Micro-Nano Energy Materials and Devices, Laboratory for Quantum Engineering and Micro-Nano Energy Technology, and Faculty of Materials and Optoelectronic Physics, Xiangtan University, Hunan 411105, P. R. China*

[b] *Institute for Superconducting and Electronic Materials (ISEM), University of Wollongong, Wollongong, NSW 2500, Australia*

[c] *Beijing Computational Science Research Center, Beijing, 100091, China*

[d] *BUAA-UOW Joint Research Centre, and School of Physics, Beihang University, Beijing, 100091, China*

[e] *State Key Laboratory of Advanced Technology for Materials Synthesis and Processing, and International School of Materials Science and Engineering, Wuhan University of Technology, Wuhan 430070, China*

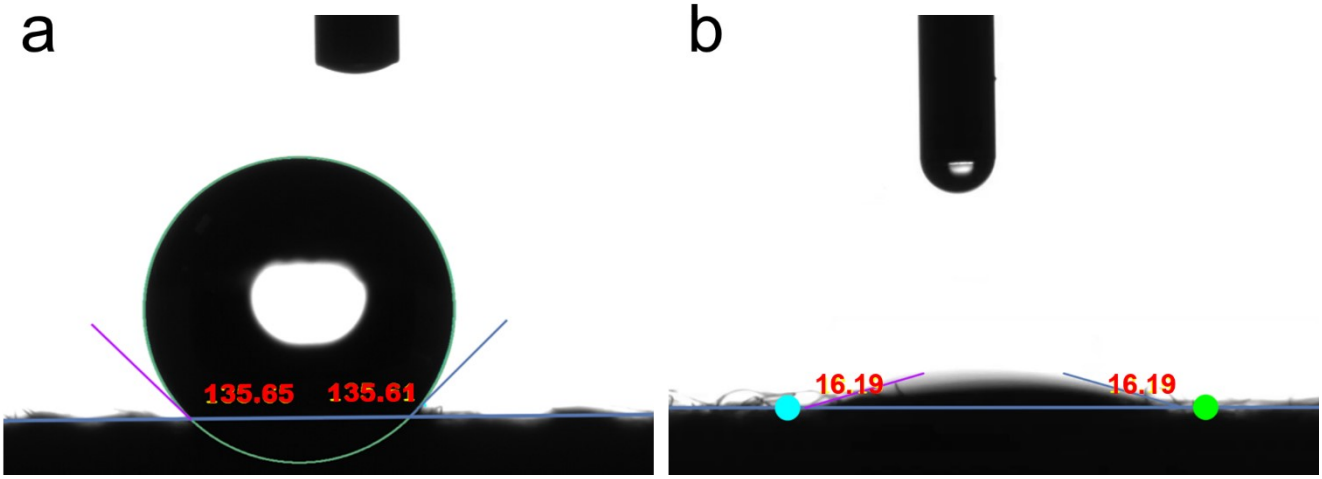

Figure S1. The water contact angles of (a) hydrophobic carbon cloth and (b) hydrophilic carbon cloth.

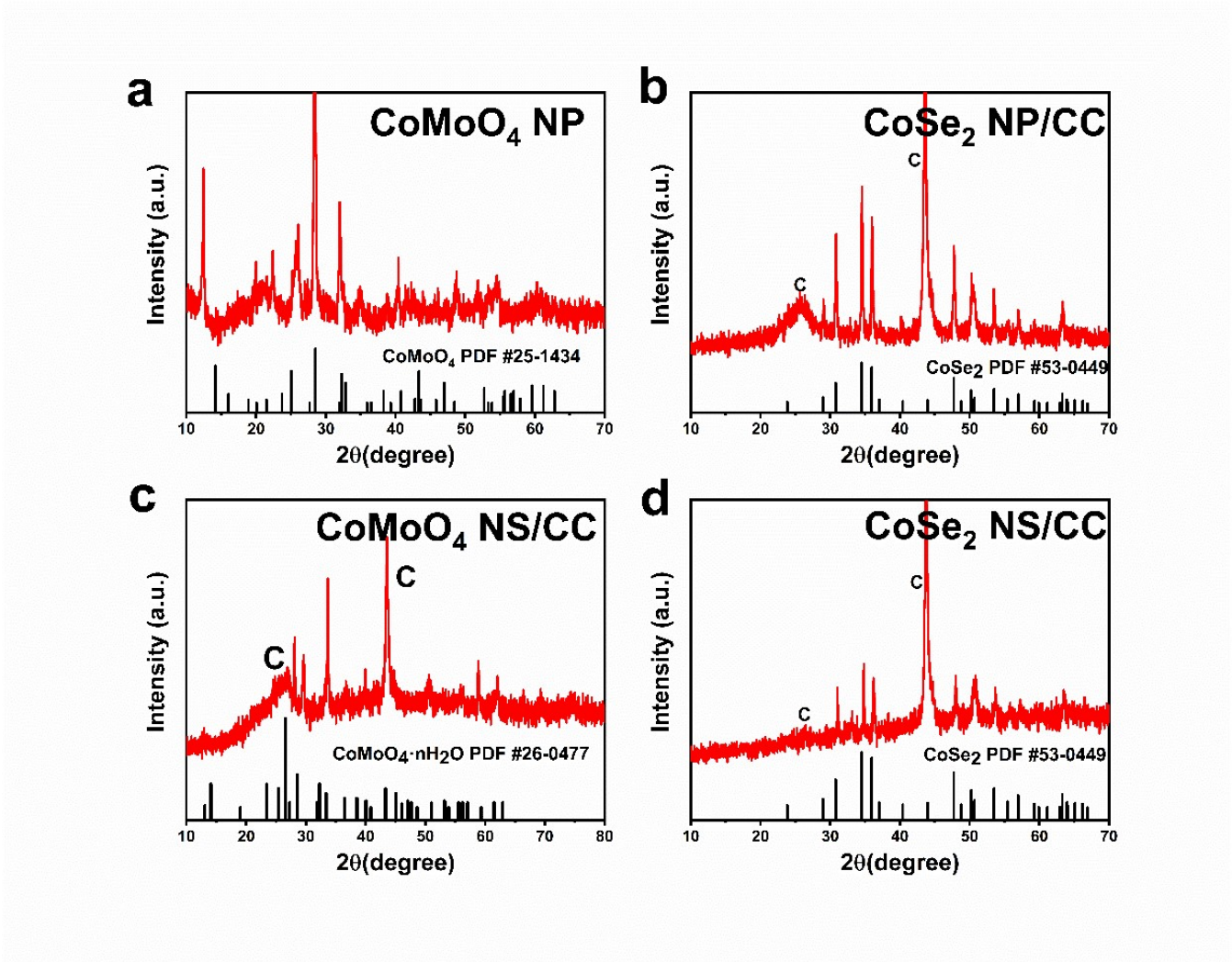

Figure S2. XRD patterns of (a) $CoMoO_4$ NP; (b) $CoSe_2$ NP/CC; (c) $CoMoO_4$ NS/CC; (d) $CoSe_2$ NS/CC.

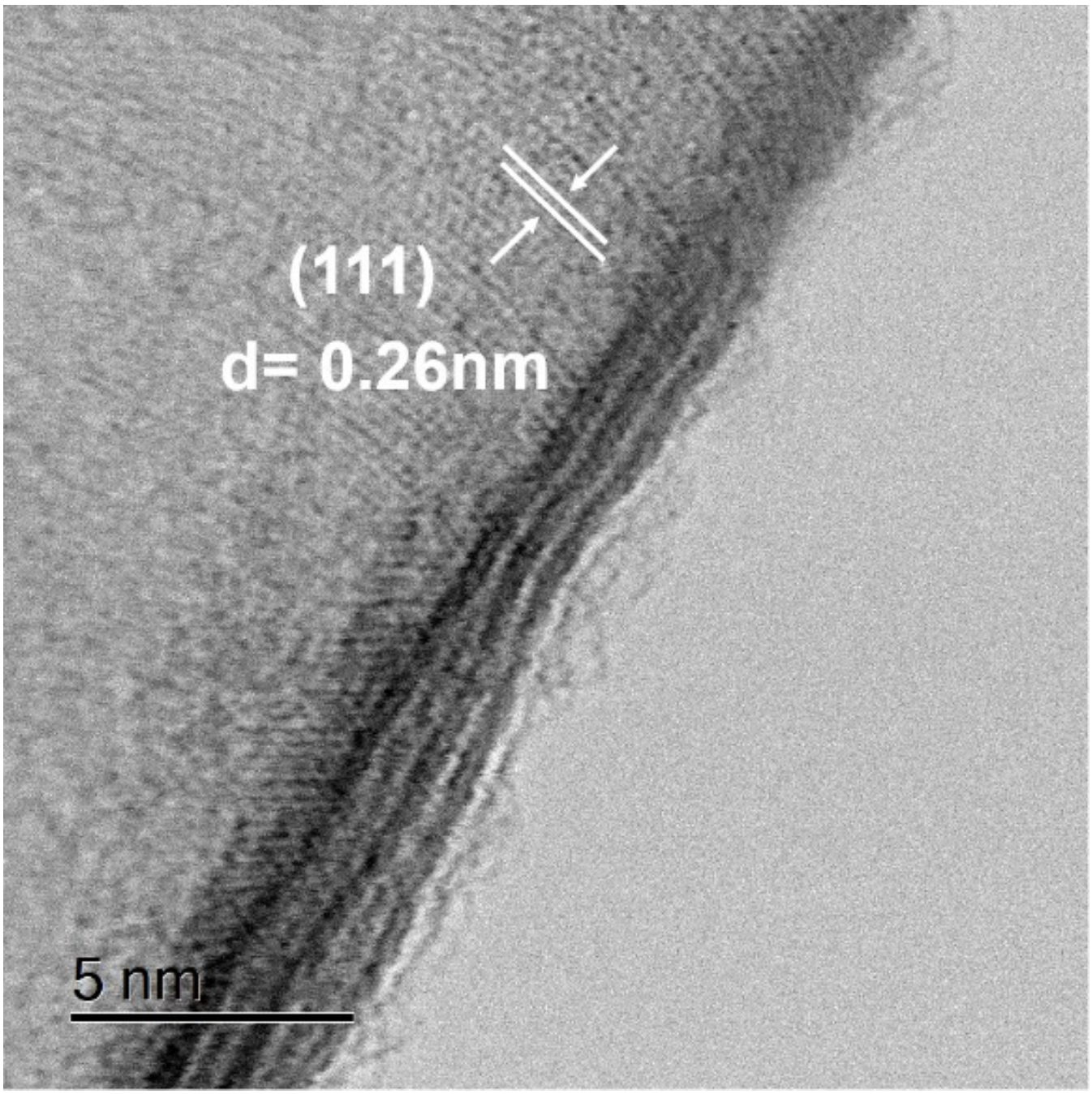

Figure S3. High-resolution TEM images of $CoSe_2$ NS/CC

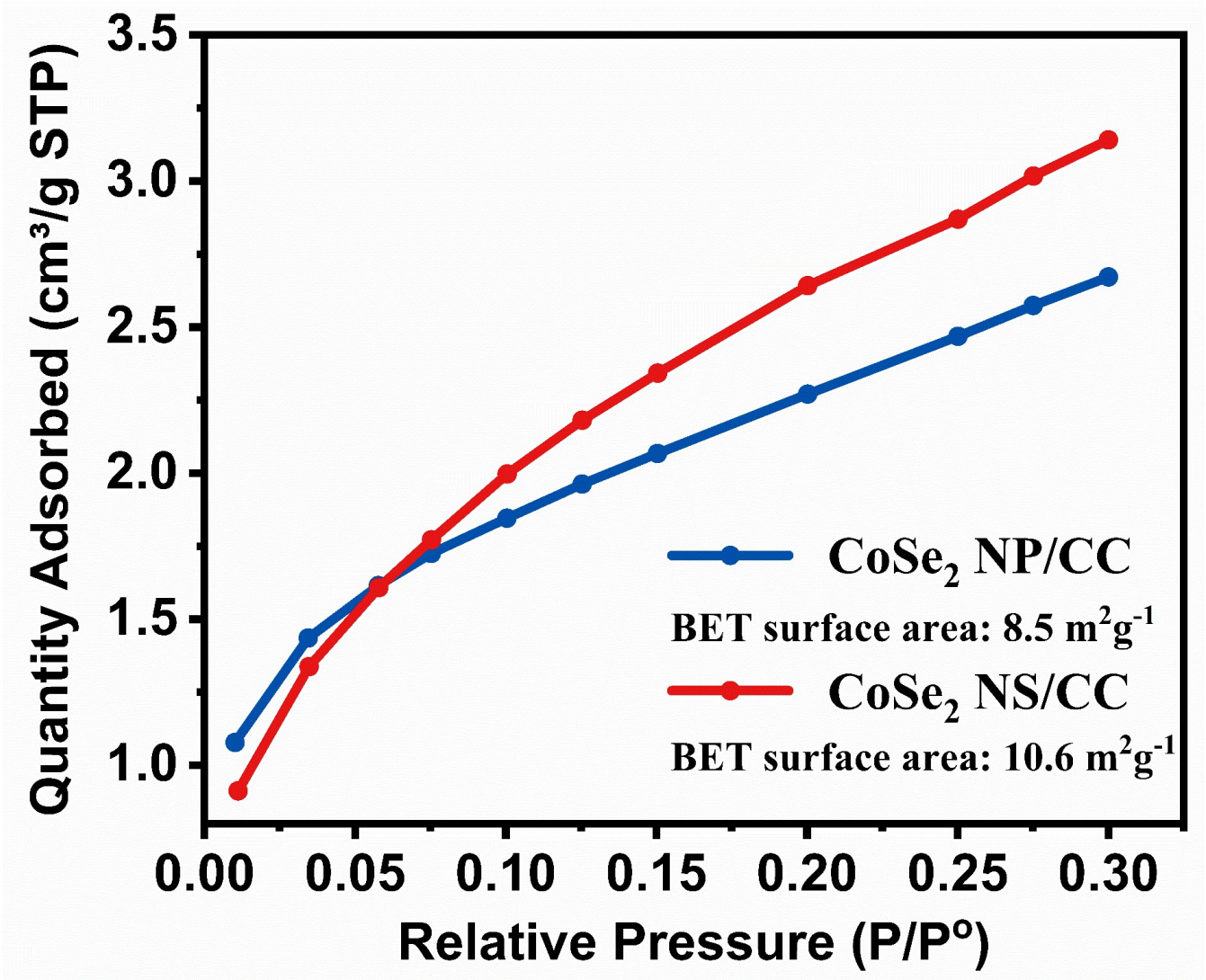

Figure S4. Nitrogen adsorption isotherms of $CoSe_2$ NS/CC and $CoSe_2$ NP/CC at 77K.

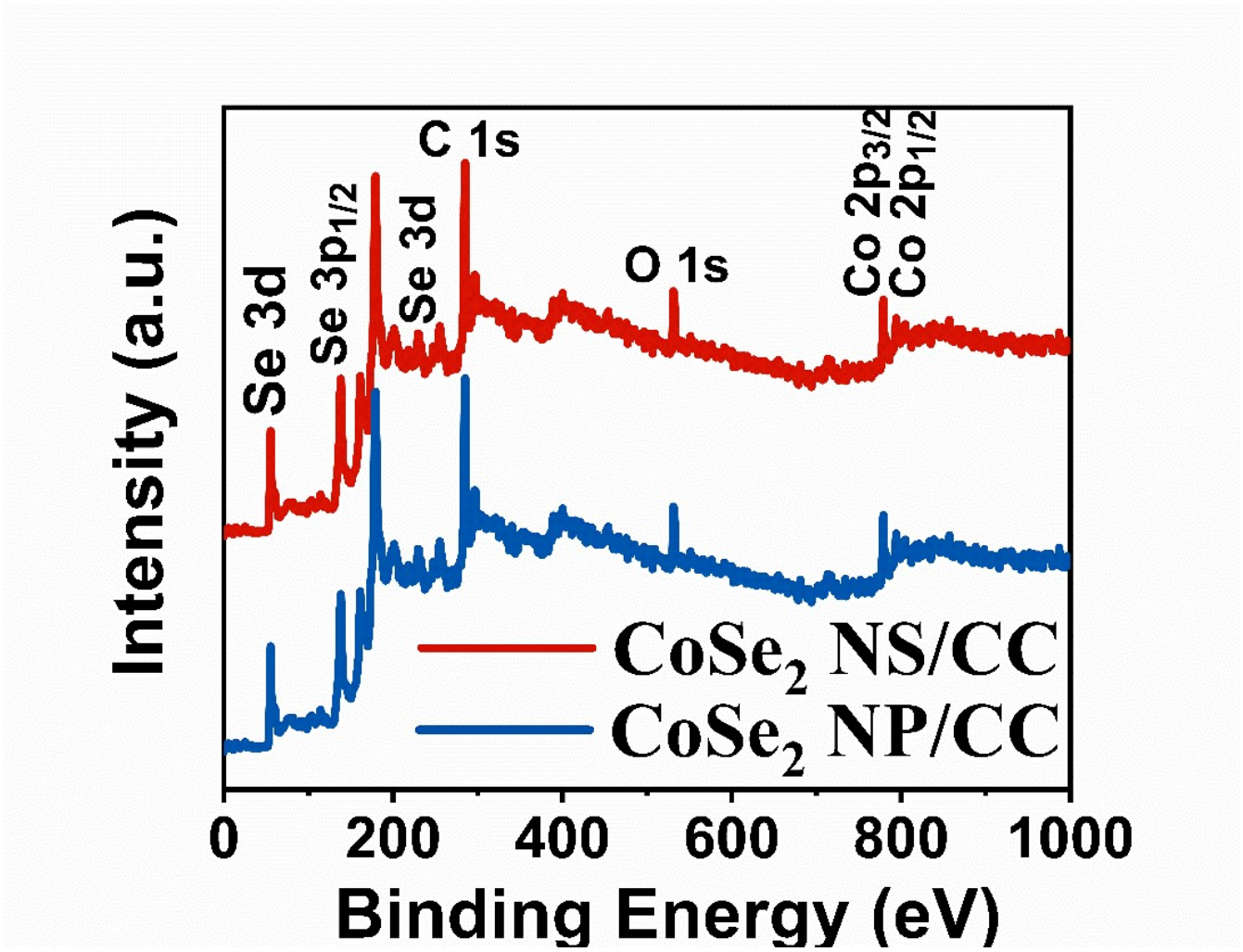

Figure S5. XPS survey spectrum of $CoSe_2$ NS/CC and $CoSe_2$ NP/CC.

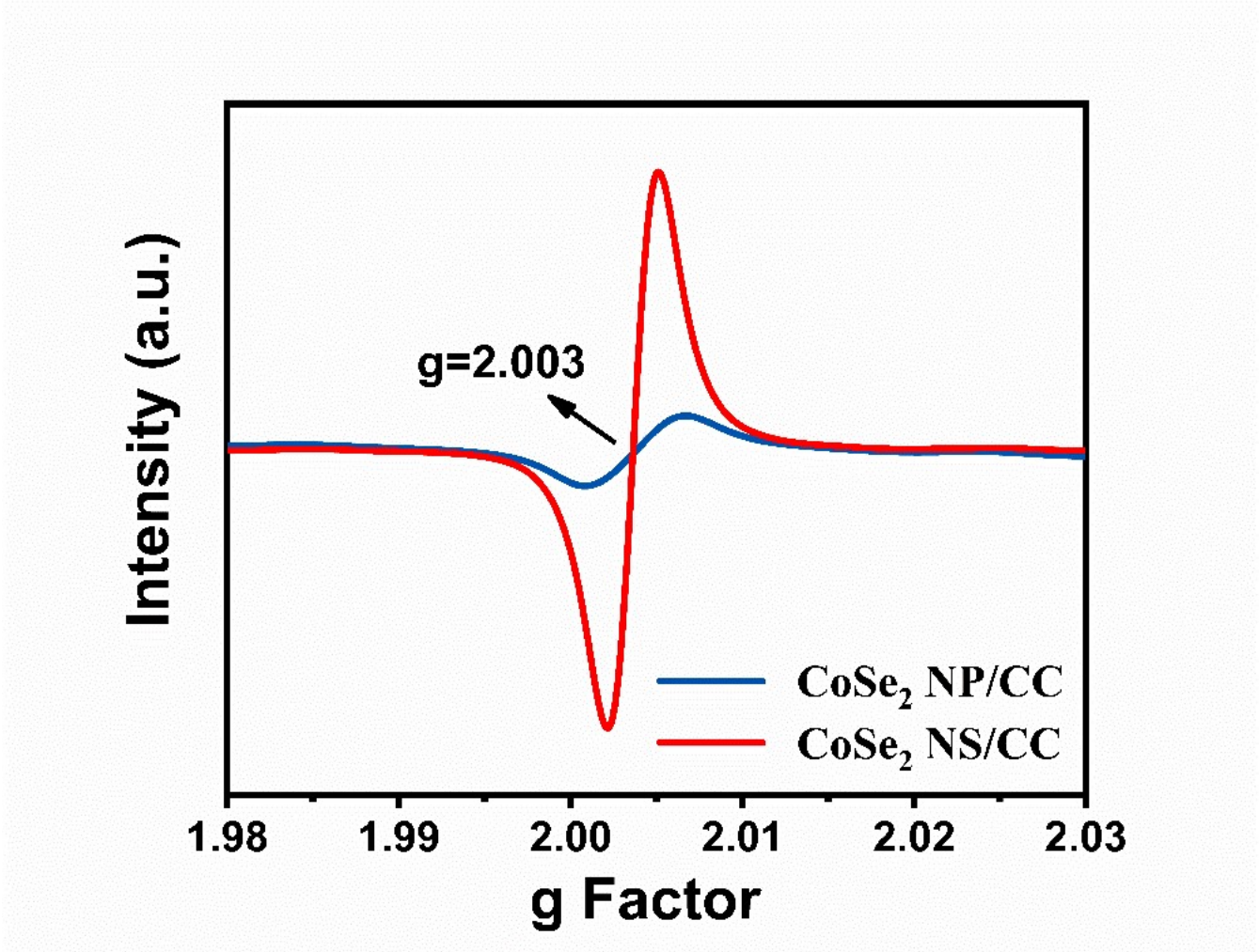

Figure S6. The EPR spectra of $CoSe_2$ NS/CC and $CoSe_2$ NP/CC.

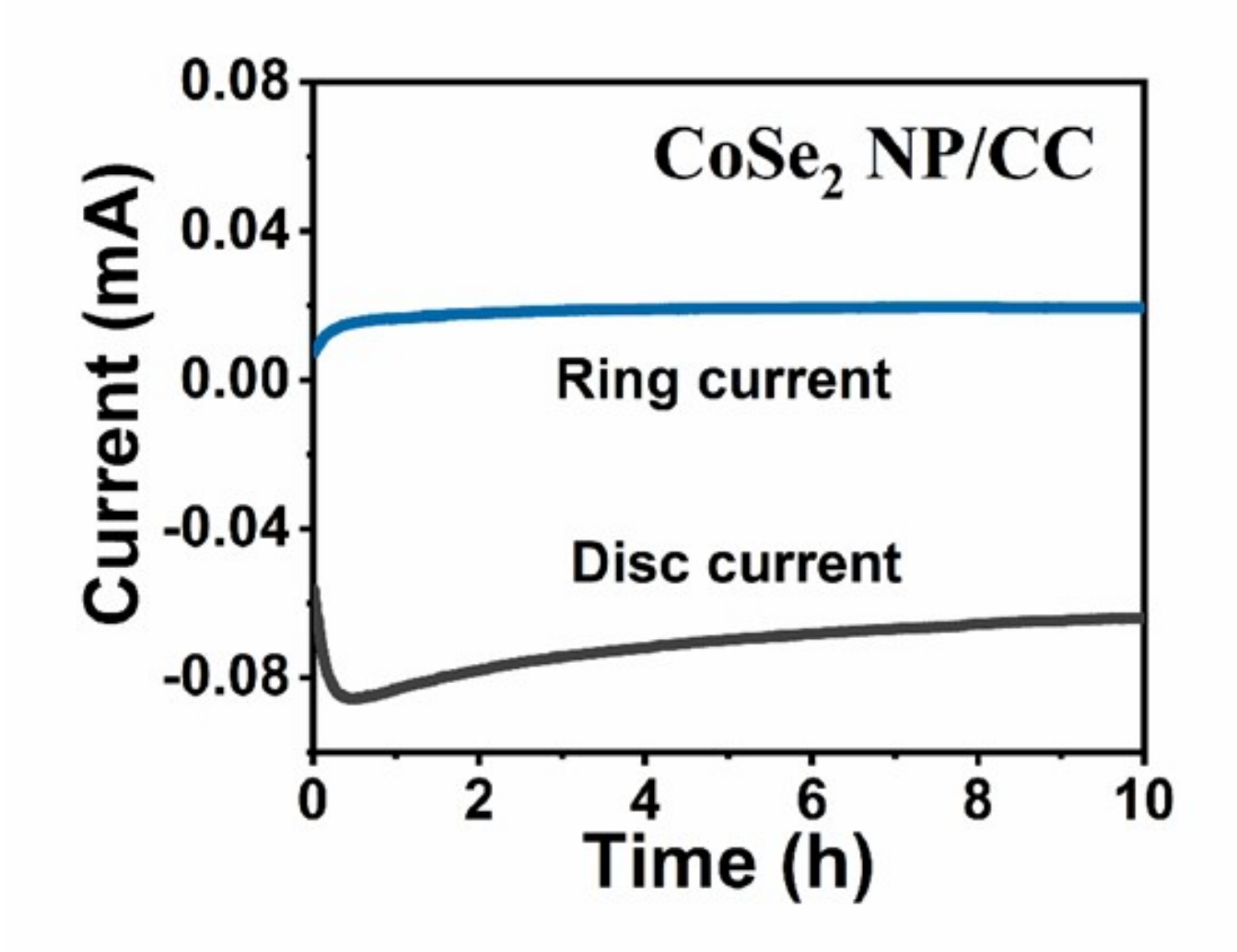

Figure S7. Stability measurements of $CoSe_2$ NP/CC at 0.1 M KOH.

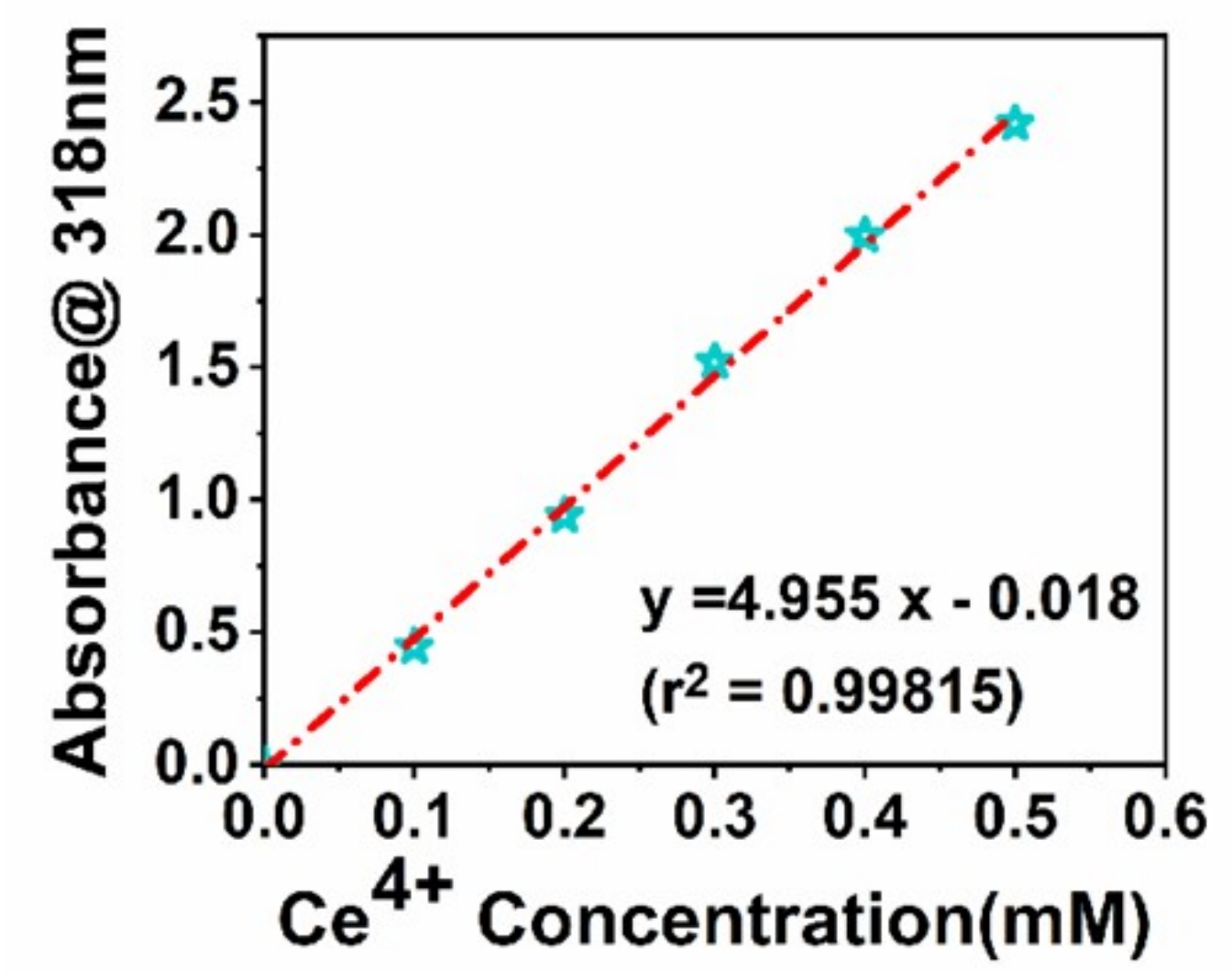

Figure S8. Linear calibration curve for UV-Visible spectra of the different concentrations of the cerium titration solution (up to 0.5 mM).

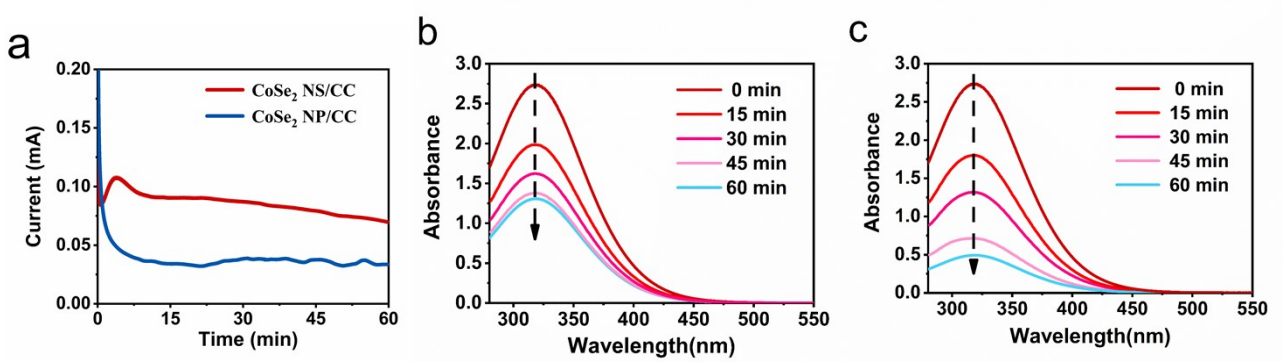

Figure S9. (a) *I–t* profile of $CoSe_2$ NS/CC and $CoSe_2$ NP/CC under a constant voltage of 0.76 V for practical H_2O_2 electrosynthesis in 0.1 M KOH solution. UV-Visible spectra indicating the generated H_2O_2 concentration every 15 min under 0.1 M KOH: (b) $CoSe_2$ NP/CC and (c) $CoSe_2$ NS/CC.

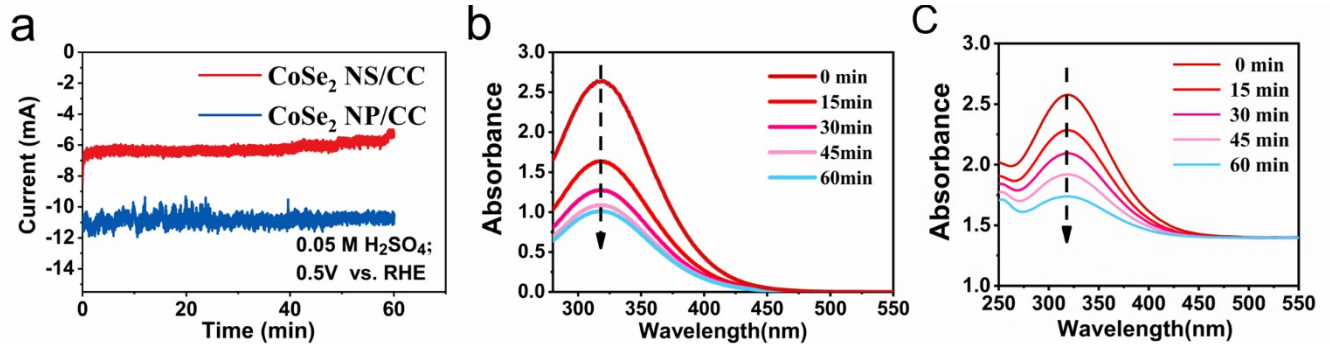

Figure S10. (a) *I–t* profile of $CoSe_2$ NS/CC and $CoSe_2$ NP/CC under a constant voltage of 0.5 V for practical H_2O_2 electrosynthesis in 0.05 M H_2SO_4 solution. UV/Visible spectra indicating the generated H_2O_2 concentration every 15 min under 0.05 M H_2SO_4: (b) $CoSe_2$ NS/CC and (c) $CoSe_2$ NP/CC.

Table S1. Activity and selectivity comparison of the $CoSe_2$ NS/CC catalyst with Co-based catalysts and precious metals for electrochemical oxygen reduction to H_2O_2.

Catalyst	Electrolyte (Volume)	Onset Potential	Selectivity	Time	Reference
$CoSe_2$ NS/CC	**0.1M KOH**	**0.72V**	**92%**	**10h**	**This work**
$CoSe_2$ NP/CC	0.1MKOH	0.71V	72%	10h	This work
Co_1−NG(O)	0.1 M KOH	0.75V	80%	110h	[1]
Co-POC-O	0.1M KOH	0.78V	84%	10h	[2]
Co−N−C	0.5M H_2SO_4	0.65V	~80%	6h	[3]
Co-NC	0.1M $HClO_4$	0.65V	>90%	10h	[4]
o-$CoSe_2$/CFP	0.05M H_2SO_4	~0.7V	83%	6h	[5]
CoS_2 nanowires	0.05M H_2SO_4	0.69V	70%	1h	[6]
Au−Pt−Ni	0.1 M KOH	0.65 V	~95%	10h	[7]

Table S2. H_2O_2 production rate comparison of various catalysts in alkaline solution.

Catalysts	Voltage	Production Rate (mg L^{-1} h^{-1})	Reference
$CoSe_2$ NS/CC	**0.76**	**1227**	**This work**
$CoSe_2$ NP/CC	0.76	782	This work
Co-POC-O	1.5	813	[2]
Ni-LDH C/CNSs	1.2	356.3	[8]
Fe-CNT	0.38	461	[9]
Co_1−NG(O)	0.58	242	[1]
aCB	0.8	20	[10]
Au−Pt−Ni	0.5	2.22	[7]

Table S3. H_2O_2 production rate comparison of various catalysts in acidic solution.

Catalysts	Voltage	Production Rate (mg L^{-1} h^{-1})	Reference
$CoSe_2$ NS/CC	**0.5**	**894**	**This work**
$CoSe_2$ NP/CC	0.5	454	This work
CoS_2	0.5	148.3	[6]
O-$CoSe_2$	0.5	90	[5]
HE-CoN/CNTs	1.2	748	[11]
g-N-CNH	0.38	1	[12]
RF-AQNC	0.1	432	[13]
Pt/HSC	0	2.65	[14]

References

1. E. Jung, H. Shin, B. H. Lee, V. Efremov, S. Lee, H. S. Lee, J. Kim, W. Hooch Antink, S. Park, K. S. Lee, S. P. Cho, J. S. Yoo, Y. E. Sung and T. Hyeon, Nat. Mater., 2020, 19, 436-442.
2. B. Q. Li, C. X. Zhao, J. N. Liu and Q. Zhang, Adv. Mater., 2019, 31, e1808173.
3. Y. Sun, L. Silvioli, N. R. Sahraie, W. Ju, J. Li, A. Zitolo, S. Li, A. Bagger, L. Arnarson, X. Wang, T. Moeller, D. Bernsmeier, J. Rossmeisl, F. Jaouen and P. Strasser, J. Am. Chem. Soc., 2019, 141, 12372-12381.
4. J. Gao, H. b. Yang, X. Huang, S.-F. Hung, W. Cai, C. Jia, S. Miao, H. M. Chen, X. Yang, Y. Huang, T. Zhang and B. Liu, Chem, 2020, 6, 658-674.
5. H. Y. Sheng, A. N. Janes, R. D. Ross, D. Kaiman, J. Z. Huang, B. Song, J. R. Schmidt and S. Jin, Energy Environ. Sci., 2020, 13, 4189-4203.
6. H. Sheng, E. D. Hermes, X. Yang, D. Ying, A. N. Janes, W. Li, J. R. Schmidt and S. Jin, ACS Catalysis, 2019, 9, 8433-8442.
7. Z. Zheng, Y. H. Ng, D.-W. Wang and R. Amal, Adv. Mater., 2016, 28, 9949-9955.
8. J. Huang, J. Chen, C. Fu, P. Cai, Y. Li, L. Cao, W. Liu, P. Yu, S. Wei, Z. Wen and J. Li, ChemSusChem, 2020, 13, 1496-1503.
9. K. Jiang, S. Back, A. J. Akey, C. Xia, Y. Hu, W. Liang, D. Schaak, E. Stavitski, J. K. Norskov, S. Siahrostami and H. Wang, Nat. Commun., 2019, 10, 3997.
10. W. Wang, Y. Hu, Y. Liu, Z. Zheng and S. Chen, ACS Appl. Mater. Interfaces, 2018, 10, 31855-31859.
11. Q. Zhang, X. Tan, N. M. Bedford, Z. Han, L. Thomsen, S. Smith, R. Amal and X. Lu, Nat. Commun., 2020, 11, 4181.
12. D. Iglesias, A. Giuliani, M. Melchionna, S. Marchesan, A. Criado, L. Nasi, M. Bevilacqua, C. Tavagnacco, F. Vizza, M. Prato and P. Fornasiero, Chem, 2018, 4, 106-123.
13. A. Wang, A. Bonakdarpour, D. P. Wilkinson and E. Gyenge, Electrochim. Acta, 2012, 66, 222-229.
14. C. H. Choi, M. Kim, H. C. Kwon, S. J. Cho, S. Yun, H. T. Kim, K. J. Mayrhofer, H. Kim and M. Choi, Nat. Commun., 2016, 7, 10922.